

# An Investigation of the Role of Quantum Statistics in Interacting Atomic and Molecular Bose–Einstein Condensates

M. K. Olsen<sup>1</sup> and L. I. Plimak<sup>2</sup>

<sup>1</sup> Instituto de Física da Universidade Federal Fluminense, Boa Viagem Cep.: 24210-340, Niterói-RJ-Brazil  
e-mail: mko@if.uff.br

<sup>2</sup> Fachbereich Physik, Universität Kaiserslautern, Kaiserslautern, 67663 Germany  
e-mail: lip@physik.uni-kl.de

Received August 29, 2003

**Abstract**—We use numerical integration of coupled differential equations in a truncated Wigner representation to show that the initial quantum state of an atomic Bose–Einstein condensate plays an important role in the process of Raman photoassociation to form a molecular condensate. Comparing the predictions for different initial quantum states, we find that, even when the stochastic prediction for an initial coherent state is close to the Gross–Pitaevskii prediction, other possible states may result in very different dynamics. The mean-field dynamics can be appreciably different, depending on the initial conditions.

## 1. INTRODUCTION

The idea of producing a molecular Bose–Einstein condensate (BEC) via Raman photoassociation of an atomic condensate has attracted much theoretical and experimental interest in the last few years. Much of the theoretical work has been performed using the Gross–Pitaevskii equation (GPE) [1], which is a semiclassical mean-field approach to the problem, or in an even more simplified fashion. That a matter wave analog of the optical processes of frequency up conversion and down conversion should exist with atomic and molecular condensates was first stated by Drummond *et al.* [2], who developed an effective quantum-field theory to describe coupled atomic and molecular BECs. An early suggestion that a molecular condensate could be produced via photoassociation came from Javanainen and Mackie [3], who proposed a two-mode, phenomenological Hamiltonian to model the process. A more complete proposal, using one atomic and two molecular fields, coupled via a two-color Raman transition so as to minimize spontaneous emission losses, was developed by Heinzen *et al.* [4]. This model was semiclassical in that it utilized a mean-field, GPE approach and hence could not predict anything about the quantum dynamics of the interacting condensates. As shown by Hope and Olsen in one dimension [5] and Hope in three dimensions [6], full quantum treatments using the positive-P representation [7, 8] may not always agree with mean-field predictions, even for the mean fields. This is not at all surprising, as it is known that the mean-field approach does not give reliable results in the optical parametric processes of second harmonic generation [9] and down conversion, the mathematical descriptions of which have many similarities to that for coupled atomic and molecular condensates. In fact, for traveling wave parametric down conversion, the mean-field prediction is that the process does not exist. How-

ever, even though previous phase-space treatments of photoassociation have been an improvement over the mean-field treatment, they all assume that the atomic BEC is initially in a coherent state. This is a natural and appealing choice in the positive-P representation as it gives a deterministic initial condition. What we will show here, however, is that the actual initial quantum state of the condensate can cause noticeable differences in the mean-field dynamics of photoassociation, even when the dynamics for an initial coherent state agrees reasonably well with the GPE predictions.

Another issue which has attracted some attention from theoreticians has been the question of the quantum state of a trapped condensate with repulsive interatomic interactions. To our knowledge, experimentalists have so far paid little attention to this issue. Perhaps the two most natural and common choices are the well-known coherent state and the number or Fock state, which are both useful in quantum optics. The coherent state is appealing because of the coherence properties exhibited [10–12], but has the problem of a largish uncertainty in number, which is conceptually difficult to understand as atoms are not created or destroyed at typical condensate temperatures. The number state is superficially an appealing choice, but, as the condensate is in contact with an environment, some particles can be added or removed. This state also has the problem that it has no defined phase. As the nonlinearity due to *s* wave collisions between condensed atoms is equivalent to a Kerr interaction, we may expect to find that the actual state is none of the above. An early calculation [13] predicted an amplitude eigenstate, while a subsequent, more rigorous calculation [14] predicted a sheared Wigner function approximating a number squeezed state. A more recent attempt, using the Hartree approximation, found a Q-function which suggests both amplitude quadrature and number squeezing [15].

In this work, we combine these two issues and consider the effects of different possible initial quantum states on the dynamics of Raman photoassociation. As the mathematics of photoassociation is essentially a more complex form of that of second harmonic generation and both quantum statistics [16, 17] and Kerr nonlinearities [18] have been shown to affect the dynamics of this process, it is of interest to investigate their effect in the present situation. Other experimental details not present in treatments of second harmonic generation are the trapping potential and the kinetic energy of the trapped condensates, both of which are included in our approach to the interacting condensates. As we are interested only in the dynamics of the mean fields rather than quantum correlations, we stochastically integrate the appropriate equations in the truncated functional Wigner representation [8, 19, 20], which we expect to give reliable results. We are not aware of any cases where this method has given predictions at variance with the full quantum solutions for field intensities, at least when the number of quanta involved are relatively large, as is the case here. This method also has the very useful advantage that numerical integration is much more stable with condensates than the functional positive-P representation, which can exhibit problems due to the large nonlinearities involved [8].

## 2. THE SYSTEM AND EQUATIONS OF MOTION

We consider that the initial atomic condensate is trapped such that one of the trapping frequencies ( $\omega_0$ ) is much smaller than the other two, leading to a cigar-shaped condensate which may reasonably be approximated as one-dimensional. We consider here a two-color Raman photoassociation scheme [4–6] coupling the ground-state atoms to a molecular condensate in the ground state via excited molecules. The excited molecular field is actually composed of multiple vibrational levels, but these excited states are essentially not populated by the Raman transition, so we treat them as a single level which will be adiabatically eliminated. In a rotating frame, the interaction part of the Hamiltonian may be written, suppressing the time dependence, as

$$\hat{H} = \frac{i\hbar}{2} \int dx (\chi(x) \hat{\Psi}_a^{\dagger 2}(x) \hat{\Psi}_{m^*}(x) - \chi(x) \hat{\Psi}_a^2(x) \hat{\Psi}_{m^*}^{\dagger}(x)) + i\hbar \int dx (\Omega(x) \hat{\Psi}_{m^*}^{\dagger}(x) \hat{\Psi}_m(x) - \Omega(x) \hat{\Psi}_{m^*}(x) \hat{\Psi}_m^{\dagger}(x)), \quad (1)$$

where  $\hat{\Psi}_a(x)$  is the atomic-field annihilation operator,  $\hat{\Psi}_{m^*}(x)$  is the excited molecular-field annihilation operator, and  $\hat{\Psi}_m(x)$  is the ground-state molecular-field annihilation operator. The Rabi frequency of the transition between atoms and excited molecules is represented by  $\chi(x)$ , and  $\Omega(x)$  is the Rabi frequency of the transition between excited- and ground-state molecules.

The first decision we must make is how to treat the quantum field problem of the two interacting condensates mathematically. Although Heisenberg equations of motion for the quantum-field operators can be written, little can be done with them as they are nonlinear operator equations for space- and time-dependent quantum fields. Another possible approach is to use the equation of motion for the density matrix. In the case of a few-mode problem with a small number of atoms, a master equation may be derived from the full Hamiltonian and then numerically integrated in the time domain. In the system under consideration here, we use an initial condensate of 20000 atoms with 1024 spatial modes. Before even considering the coupling with the molecular condensate, the master equation approach would need a Hilbert space of dimension  $1024^{20000}$ , which is clearly intractable. We will therefore resort to the use of a phase-space representation, which allows mapping of the quantum Hamiltonian onto stochastic differential equations for complex variables and allows for numerical stochastic integration of the resulting equations. This approach was first used to calculate correlation functions for a one-dimensional trapped condensate [8] and shortly thereafter to model the process of evaporative cooling [21].

The process of photoassociation has previously been treated using a functional positive-P representation [5, 6] with adiabatic elimination of the excited molecules, which gives true stochastic differential equations for the coupled atomic and molecular fields. However, numerical integration of these equations is very time consuming and can present serious stability problems [8]. Hence we will use a truncated functional Wigner representation, which is much more stable and lends itself more readily to the modeling of different initial quantum states of the atomic condensate. A full Wigner representation of this problem would have derivatives of third order in the equation of motion for the pseudoprobability function, coming from both the interaction Hamiltonian above and the self-interaction terms. While it is possible to model these using stochastic difference equations [22], there are severe practical difficulties involved. However, as is commonly done with the Wigner representation, we can discard the third-order derivatives, which in this case leaves us with a functional Fokker–Planck equation with no diffusion matrix. This can be immediately mapped onto differential equations which have the appearance of coupled Gross–Pitaevskii-type equations. It must be stressed that there are, however, two important differences. Firstly, averages must be taken over a large number of integrations of these equations, with initial conditions chosen so as to represent the Wigner function for the desired initial quantum states. Only if the Wigner function were to be a Dirac delta, which is completely nonphysical, would we recover the Gross–Pitaevskii equations. It is the probabilistic distribution of the initial state that allows the evolution of complex variables to represent (to a very good approximation)

the evolution of noncommuting field operators. Secondly, being an approximation to the full Wigner representation, the truncated Wigner representation yields symmetrically ordered operator averages [23]. Formulae for physical quantities which are expressed as normally ordered operator averages must be corrected due to the operator reordering, as is done in Eq. (5) below. In this paper, we are only interested in single-time averages, so the free commutation relations for the field operators are sufficient. In general, the problem of reordering Heisenberg operators for different times may be tackled using methods developed in [23], as was done previously to calculate the symmetrized products needed for QND measurements [24]. With these reservations in mind, we can now model the quantum fields via equations which are completely classical in appearance.

Using the same units as Cusack *et al.* [25], with time measured in units of  $\omega_0^{-1}$  and space in units of  $\sqrt{\hbar/m\omega_0}$ , we are then able to describe the process using two coupled equations for the complex atomic ( $\Psi_a$ ) and molecular ( $\Psi_m$ ) fields, with the spatial and temporal dependences neglected for notational convenience:

$$\begin{aligned} i\frac{\partial\Psi_a}{\partial t} &= -\frac{\partial^2\Psi_a}{\partial x^2} + V_a(x)\Psi_a \\ &+ (U_{aa}|\Psi_a|^2 + U_{am}|\Psi_m|^2)\Psi_a + i\kappa\Psi_a^*\Psi_m, \\ i\frac{\partial\Psi_m}{\partial t} &= -\frac{1}{2}\frac{\partial^2\Psi_m}{\partial x^2} + V_m(x)\Psi_m \\ &+ (U_{mm}|\Psi_m|^2 + U_{am}|\Psi_a|^2 - \Delta)\Psi_m - \frac{i}{2}\kappa\Psi_a^2. \end{aligned} \quad (2)$$

In the above,  $V_a(x)$  ( $V_m(x)$ ) represents the trapping potential for the atomic (molecular) condensate,  $U_{aa}$  is the atom–atom interaction strength,  $U_{mm}$  represents that between molecules, and  $U_{am}$  represents atom–molecule scattering, all in the  $s$  wave  $\delta$ -function approximation. The coupling strength  $\kappa$ , chosen as real and spatially constant here, is now the effective two-photon Rabi frequency, while  $\Delta$  is the effective two-photon Raman detuning. In this model, we ignore spontaneous losses and interactions with the thermal cloud, which does not exist in our zero-temperature treatment.

### 3. RESULTS

For the purposes of comparison, in all simulations we use as our starting point a ground-state solution of the GPE for a one-dimensional trapped atomic condensate with  $2 \times 10^4$  atoms and a value of the nonlinear interaction of  $U_{aa} = 4 \times 10^{-3}$ . This initial solution is obtained via propagation in imaginary time [26], beginning with the Thomas–Fermi solution for these param-

eters. In all our investigations, we use  $U_{am} = -1.5U_a$ ,  $U_{mm} = 2U_{aa}$ ,  $\kappa = 1$ ,  $\Delta = 0$ , and a molecular trapping potential twice that of the harmonic atomic potential, all consistent with [25]. The difference between the molecular and atomic trapping potentials, given the same magnetic spin, comes directly from the increased mass of the molecules. The integration always begins with all particles in the atomic condensate and a coherent vacuum for the molecular field. The equations are integrated over  $10^4$  trajectories using a standard split-operator method with momentum propagation in the Fourier space and a three-step predictor–corrector method in position space. It is readily seen that the grid spacing  $\Delta x$  has to be chosen larger than the magnitude of the  $s$  wave scattering lengths, effectively becoming a momentum cutoff. With  $\Delta x$  too small, we would encounter ultraviolet divergences, these being even more calamitous in higher dimensions. The accuracy and stability of the integration is checked by keeping track of the conserved quantity of the number of atoms plus two times the number of molecules,  $N_a + 2N_m$ , and also by varying the time step. Over the times shown,  $t = \pi/16$ , results with a halved time step were virtually indistinguishable from those shown and the number was conserved to within less than 0.05%.

To model the quantum states of the condensates, each of the 1024 points in the spatial grid is given an initial value on each trajectory, chosen from the Wigner distribution for the appropriate state. A coherent state is modeled by taking the (real) GPE solution for the  $n$ th spatial point and adding real and imaginary numbers drawn from a normal Gaussian distribution, giving  $\Psi(x_n) = \Psi_{GP}(x_n) + 0.5(\eta_1 + i\eta_2)/\sqrt{\Delta x}$ . It is easily verified that the trajectory average will be  $|\Psi_{GP}(x_n)|^2 + 1/2\Delta x$  at each point, with  $1/2\Delta x$  needing to be subtracted at each point once the trajectory averaging has taken place. A minimum uncertainty squeezed state is modeled by adding  $0.5(\eta_1 e^{-r} + i\eta_2 e^r)/\sqrt{\Delta x}$  at each point, where  $r$  is the squeezing parameter. A positive  $r$  gives squeezing in the amplitude quadrature, while a negative  $r$  gives phase quadrature squeezing. A sheared state, typical of Kerr nonlinearities, as in Dunningham *et al.* [14], is simulated by transforming the added squeezed-state noise by a factor  $\exp(iq\eta_3)$ , where  $q$  is the shearing factor. The real noise terms used above have the correlations

$$\overline{\eta_j} = 0, \quad \overline{\eta_i\eta_j} = \delta_{ij}. \quad (3)$$

Numerical checks of single-mode distributions produced using these methods show that they give the expected values for both average numbers and quadrature variances. In our simulations for squeezed states, we use values of  $r = \pm \log 0.5$ , while for the sheared state we used  $q = 0.005$ , which gives results similar to the Wigner function shown in [14]. We also investigate a more extreme shearing of the distribution, with  $r = -\log 0.2$  and  $q = 0.05$ , as we are treating a larger con-

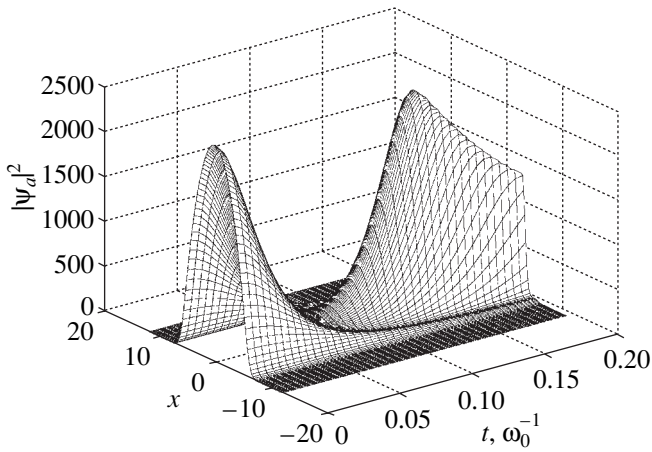


**Fig. 1.** GPE atomic-field prediction up to  $t = \pi/16$  showing the spatial dynamics of the atomic BEC, which is not calculable in a single-mode approach. The units of the spatial axis are  $\sqrt{\hbar/m\omega_0}$ .

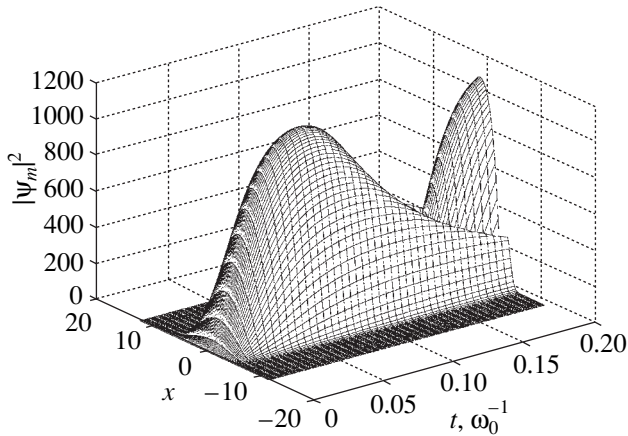


**Fig. 2.** GPE molecular-field prediction up to  $t = \pi/16$ .

condensate than those considered in [14, 15]. This state, which we call a crescent state, will have a larger effective Kerr nonlinearity and thus will be expected to have a more sheared Wigner distribution. This is the state we consider the most likely of the above options for the initial atomic condensate. The molecular field always begins as a coherent vacuum.

We begin by numerically integrating the GPE type equations, which give semiclassical results with the quantum statistics playing no part in the time evolution. These results are then used for purposes of comparison with the results of the truncated Wigner representation. What we find is that the spatial dependence of the trapped condensates plays an important role in the process, with the coupling rates at different densities being

different. For the parameters used, this causes an interesting structure to emerge, with spatial sidebands forming in the distributions, as shown in Figs. 1 and 2. Over the times shown here, the kinetic energy of the condensates plays a negligible role, with integration of spatially separate single-mode equations at each spatial point giving virtually identical predictions, both spatially and for the total particle numbers. This is not the case for longer interaction times, where the full spatial problem needs to be solved.

Examining Figs. 3 and 4, which show the mean particle numbers, we see that when we use an initial coherent state in the Wigner equations, we do not see the dramatic differences from the GPE predictions reported previously [5, 6]. The reason is simply that we are working with different parameters, with the ratio between  $\kappa$  and the strength of the nonlinear interactions being important in this regard. This was previously demonstrated to be the case in traveling wave second harmonic generation with additional  $\chi^{(3)}$  nonlinearities. Although this is not as rich a system as coupled condensates, a useful analogy can be made [18]. Initial states with the degree of amplitude squeezing and shearing as calculated in [14, 15] also do not lead to vastly different predictions, the difference between the two being almost negligible. However, a dramatic difference occurs when we consider the initial crescent state, which is greatly sheared in phase space with a large degree of number squeezing (the single-mode Fano factor for this distribution is approximately 0.2) but is well above the minimum uncertainty product in the quadratures (single-mode  $V(X) \approx 0.6$ ,  $V(Y) \approx 15$ ).

It seems that the differences seen are largely not due to the spatial intensity correlation, defined using the field operators as

$$g^{(2)}(x, x) = \frac{\langle \hat{\Psi}_a^\dagger(x) \hat{\Psi}_a^\dagger(x) \hat{\Psi}_a(x) \hat{\Psi}_a(x) \rangle}{\langle \hat{\Psi}_a^\dagger(x) \hat{\Psi}_a(x) \rangle^2}, \quad (4)$$

which is predicted to affect the initial conversion rate for second harmonic generation [16, 17] and condensates in free space [27]. In the variables of the Wigner representation, which represent symmetrically ordered operator averages, the definition is

$$g^{(2)}(x, x) = \frac{|\overline{\Psi_a(x)}|^4 - 2|\overline{\Psi_a(x)}|^2 + 1/2\Delta x}{(|\overline{\Psi_a(x)}|^2 - 1/2\Delta x)^2}. \quad (5)$$

This factor varies between 1 and 1.04 at the center for the initial states considered here, and the initial conversion rate remains almost unchanged. The differences come in the first minimum of the atomic population and in subsequent revivals and are more readily explained by the degree of phase uncertainty in the initial state. It can be seen by examining Eq. (2) that whether association or disassociation is predominant will depend on the phase of the products  $\Psi_a^* \Psi_m$  and  $\Psi_a^2$ . As the crescent

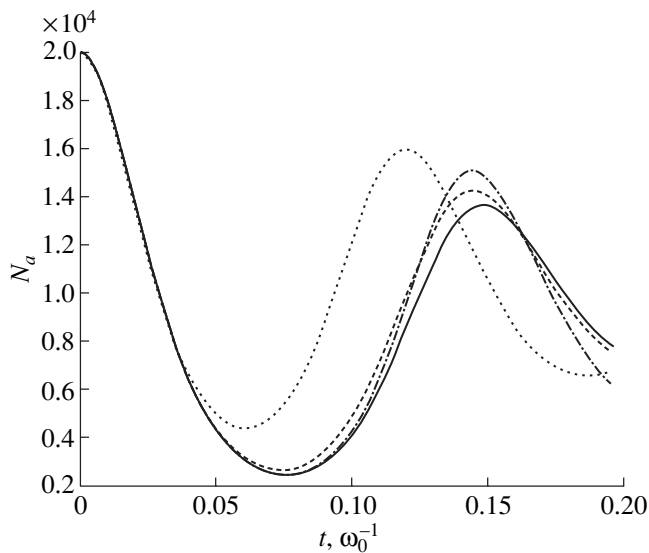


**Fig. 3.** Atomic population predictions. The dash-dotted line is the GPE solution, the solid line is for an initial coherent state, the dashed line is the amplitude squeezed state, and the dotted line is the more highly sheared crescent state.

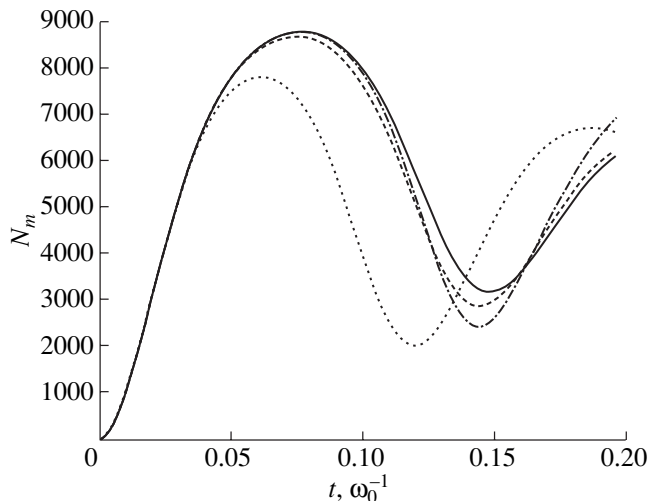


**Fig. 4.** Molecular population predictions, with lines as in Fig. 3.

state has a larger phase uncertainty than the others considered here, the photodissociation process begins to dominate and the mean number of atoms begins to revive at an earlier time than for the other states. This result tends to suggest that the closer the initial atomic state to a number state, the more markedly different the predictions may be and the more important it will be to take quantum effects into consideration. Unfortunately, a number state has a Wigner function expressed in terms of Laguerre polynomials [28], which is not easy to model numerically for the atom numbers considered in this work.

#### 4. CONCLUSIONS

We have demonstrated that care must be taken in making theoretical predictions for the process of Raman photoassociation used to couple atomic and molecular Bose–Einstein condensates. Calculations in the mean-field approach using the Gross–Pitaevskii equation cannot be relied on to give accurate predictions. Using numerical stochastic integrations of the field equations in a truncated Wigner representation, we have shown that the quantum state of the initial atomic condensate plays an important role in the mean-field dynamics of the two interacting fields. We have shown how different initial quantum states can give quite different results even when the GPE predicts the dynamics for an initial coherent state reasonably accurately. All the quantum states considered gave some difference from the GPE predictions, but the crescent state, possibly the most likely for BEG, is the most dramatic, showing a markedly less complete conversion to molecules. Over the time scales we considered, the quantum statistics are much more important than the spatial dependence of the condensate. These results suggest that, for the purposes of Raman photoassociation, a careful preparation of the initial atomic condensate will be important for the resulting dynamics and that any calculations aimed at predicting the process accurately will need to take quantum statistics into account.

#### ACKNOWLEDGMENTS

This research was supported by the New Zealand Foundation for Research, Science and Technology (UFRJ0001) and the Deutsche Forschungsgemeinschaft under contract FL210/11.

#### REFERENCES

1. F. Dalfovo *et al.*, *Rev. Mod. Phys.* **71**, 463 (1999).
2. P. D. Drummond, K. V. Kheruntsyan, and H. He, *Phys. Rev. Lett.* **81**, 3055 (1998).
3. J. Javanainen and M. Mackie, *Phys. Rev. A* **59**, R3186 (1999).
4. D. J. Heinzen *et al.*, *Phys. Rev. Lett.* **84**, 5029 (2000).
5. J. J. Hope and M. K. Olsen, *Phys. Rev. Lett.* **86**, 3220 (2001).
6. J. J. Hope, *Phys. Rev. A* **64**, 053608 (2001).
7. P. D. Drummond and C. W. Gardiner, *J. Phys. A* **13**, 2353 (1980).
8. M. J. Steel *et al.*, *Phys. Rev. A* **58**, 4824 (1998).
9. M. K. Olsen *et al.*, *Phys. Rev. A* **61**, 021 803 (2000).
10. M. R. Andrews *et al.*, *Science* **275**, 637 (1997).
11. W. Ketterle and H. J. Miesner, *Phys. Rev. A* **56**, 3291 (1997).
12. J. M. Vogels, J. K. Chin, and W. Ketterle, *Phys. Rev. Lett.* **90**, 030403 (2003).
13. M. Lewenstein and L. You, *Phys. Rev. Lett.* **77**, 3489 (1996).

14. J. A. Dunningham, M. J. Collett, and D. F. Walls, *Phys. Lett. A* **245**, 49 (1998).
15. J. Rogel-Salazar, S. Choi, G. H. C. New, and K. Burnett, *Phys. Lett. A* **299**, 476 (2002).
16. Y. R. Shen, *Phys. Rev.* **155**, 921 (1967).
17. M. K. Olsen, L. I. Plimak, and A. Z. Khoury, *Opt. Commun.* **201**, 373 (2002).
18. V. I. Kruglov and M. K. Olsen, *Phys. Rev. A* **64**, 053802 (2001).
19. A. Sinatra, C. Lobo, and Y. Castin, *Phys. Rev. Lett.* **87**, 210404 (2001).
20. A. Sinatra, C. Lobo, and Y. Castin, *J. Phys. B: At. Mol. Opt. Phys.* **35**, 3599 (2002).
21. P. D. Drummond and J. F. Corney, *Phys. Rev. A* **60**, 2661 (1999).
22. L. I. Plimak, M. K. Olsen, M. Fleischhauer, and M. J. Collett, *Europhys. Lett.* **56**, 372 (2001).
23. L. I. Plimak, M. Fleischhauer, M. K. Olsen, and M. J. Collett, *cond-mat/0102483* (2001).
24. M. K. Olsen, L. I. Plimak, M. J. Collett, and D. F. Walls, *Phys. Rev. A* **62**, 023802 (2000).
25. B. J. Cusack, T. J. Alexander, E. A. Ostrovskaya, and Y. S. Kivshar, *Phys. Rev. A* **65**, 013609 (2001).
26. H. Wallis, A. Röhl, M. Naraschewski, and A. Schenzle, *Phys. Rev. A* **55**, 2109 (1997).
27. K. V. Kheruntsyan, D. M. Gangardt, P. D. Drummond, and G. V. Shlyapnikov, *Phys. Rev. Lett.* **91**, 040 403 (2003).
28. C. W. Gardiner, *Quantum Noise* (Springer, Berlin, 1991).